European Conference on Computational Fluid Dynamics
ECCOMAS CFD 2006
P. Wesseling, E. Oñate and J. Périaux (Eds)

MAGNETOHYDRODYNAMICS IN A FINITE CYLINDER: POLOIDAL-TOROIDAL DECOMPOSITION

Piotr Boronski* **and Laurette S. Tuckerman†**

*Center for Turbulence Research
Stanford University, Bldg. 500, Stanford, CA 94305-3035
e-mail: boronski@stanford.edu
†Laboratoire d'Informatique pour la Mécanique et les Sciences de l'Ingénieur
LIMSI-CNRS, B.P. 133, F-91403 Orsay France
e-mail: laurette@limsi.fr
web page:http://www.limsi.fr/Individu/laurette

Key words: incompressibility, poloidal-toroidal, magnetohydrodynamics, Green functions, influence matrix

Abstract. *The magnetohydrodynamic equations present two challenging algorithmic requirements: that both fields be solenoidal and that the magnetic field match an unknown external field. The poloidal-toroidal decomposition represents a three-dimensional solenoidal vector field via two scalar potentials. Widely used in Cartesian and spherical geometries with periodic boundary conditions, complications appear in finite geometries which can, however, be circumvented. An implementation of the poloidal-toroidal decomposition for the magnetohydrodynamic equations in a finite cylinder is described, which uses a spectral spatial discretisation. A Green's function method is proposed for matching the magnetic field in a spectral representation to an external field in a vacuum.*

1 Poloidal-toroidal decomposition

The requirement that velocity and magnetic fields be solenoidal, i.e. divergence-free, represents one of the most challenging difficulties in hydrodynamics and in magnetohydrodynamics. This condition is the approximation used in incompressible fluid dynamics, and is the statement of the non-existence of magnetic monopoles in electromagnetism.

Two main approaches exist for satisfying this requirement. The first method is to conserve three field components and to project three-dimensional fields onto divergence-free fields. Indeed, in an incompressible fluid, the pressure serves only to counterbalance the nonlinear term which is the source of the divergence in the Navier-Stokes equations. The pressure also plays this role numerically. The divergence of the Navier-Stokes equations is taken, leading to a Poisson problem for the pressure. However, the boundary conditions on the equations for $(\mathbf{u}, p)$ involve only the velocity, leading to coupling between the equations to be solved for $\mathbf{u}$ and p. In projection-diffusion schemes, approximate boundary conditions are imposed for the pressure.

Otherwise, the coupled equations are solved in several stages by a Green's function or influence matrix method [1].

In contrast, for magnetic fields, the exact evolution of the equations conserves divergence and there exists no analog to the pressure. Thus if the numerical algorithm creates divergence, there is no mechanism for eliminating it and it may accumulate [2]. For this reason, magneto-hydrodynamic codes sometimes include a fictitious magnetic pressure, which must be treated numerically.

The other possibility is to express fields in such a way that they are divergence-free by construction. More specifically, in a simply connected domain, a solenoidal $\mathbf{F}$ can be written as

$$\mathbf{F} = \nabla \times (\psi \hat{\mathbf{e}}) + \nabla \times \nabla \times (\phi \hat{\mathbf{e}}) \tag{1}$$

where $\hat{\mathbf{e}}$ denotes a unit vector. Figure 1 shows the vector field resulting from poloidal (ϕ) and toroidal (ψ) potentials in our case of a cylindrical geometry and $\hat{\mathbf{e}} = \hat{\mathbf{e}}_z$, for an axisymmetric field.

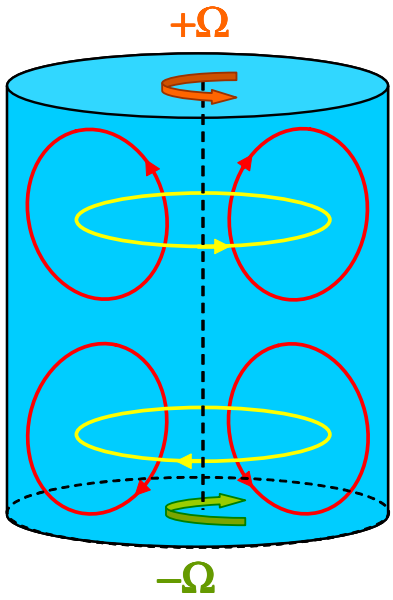

Figure 1: The topological flow structures in the case of counter-rotating disks: red (dark) – poloidal (ϕ) flow lines, yellow (light) – toroidal (ψ) flow lines.

The advantage of (1) is that $\mathbf{F}$ is divergence-free by construction and involves only two scalar fields. The poloidal-toroidal decomposition lends itself particularly well to geometries in which $\hat{\mathbf{e}}$ (which we will call vertical) can be taken to be normal to the physical boundaries and the horizontal directions (those perpendicular to $\hat{\mathbf{e}}$) are periodic. Standard examples are a spherical geometry with $\hat{\mathbf{e}} = \hat{\mathbf{e}}_\rho$ [3, 4] or a three-dimensional Cartesian geometry with one bounded direction along $\hat{\mathbf{e}}$ and two periodic directions, such as channel flow [5].

2 Governing equations

Evolution operators for the potentials ψ and ϕ are derived by taking successive normal components and curls, since these operations extract the potentials. For $\hat{\mathbf{e}} = \hat{\mathbf{e}}_z$ (or $\hat{\mathbf{e}} = \hat{\mathbf{e}}_\rho$ in spherical coordinates),

$$\begin{aligned} \hat{\mathbf{e}} \cdot \mathbf{F} &= -\Delta_h \phi, & \text{(2a)} \\ \hat{\mathbf{e}} \cdot \nabla \times \mathbf{F} &= -\Delta_h \psi, & \text{(2b)} \\ \hat{\mathbf{e}} \cdot \nabla \times \nabla \times \mathbf{F} &= \Delta \Delta_h \phi. & \text{(2c)} \end{aligned}$$

where Δ_h is the two-dimensional horizontal Laplacian.

Our application to a finite cylinder is based on the treatment by Marques [6, 7], Equations (2) hold for $\hat{\mathbf{e}} = \hat{\mathbf{e}}_z$ (but not for $\hat{\mathbf{e}} = \hat{\mathbf{e}}_r$). The horizontal direction θ is periodic, but r is not. The increase in order of the equations in r must be compensated for by additional boundary conditions. One of these is a gauge condition lifting the non-uniqueness of the representation (1). The other is a compatibility condition analogous to a constant of integration and arises from the differentiation used in (2). Marques [6] proved that, for $\mathbf{g}$ defined over a simply connected domain Ω, the equation:

$$\mathbf{g} = 0 \quad \text{in } \Omega \tag{3}$$

is equivalent to:

$$\begin{aligned} \hat{\mathbf{e}} \cdot \mathbf{g} = 0 \qquad & \text{in } \Omega & \text{(4a)} \\ \hat{\mathbf{e}} \cdot \nabla \times \mathbf{g} = 0 \qquad & \text{in } \Omega & \text{(4b)} \\ \nabla \cdot \mathbf{g} = 0 \qquad & \text{in } \Omega & \text{(4c)} \\ \hat{\mathbf{n}} \cdot \mathbf{g} = 0 \qquad & \text{on } \partial\Omega_h & \text{(4d)} \end{aligned}$$

where $\hat{\mathbf{n}}$ is the vector normal to the boundary $\partial\Omega_h$ of slices perpendicular to $\hat{\mathbf{e}}$. (In our case with $\hat{\mathbf{e}} = \hat{\mathbf{e}}_z$, the slices Ω_h are disks, their boundaries $\partial\Omega_h$ are circles, and $\hat{\mathbf{n}} = \hat{\mathbf{e}}_r$ is the radial unit vector.) Equation (4c) requires that $\mathbf{g}$ be solenoidal and equation (4d) is the compatibility condition.

We now wish to apply (4) to the magnetohydrodynamic equations:

$$\begin{aligned} \left(\partial_t - \frac{1}{Re}\Delta\right)\mathbf{u} + (\mathbf{u}\cdot\nabla)\mathbf{u} - (\mathbf{B}\cdot\nabla)\mathbf{B} &= -\nabla(p + \frac{B^2}{2}) & \text{(5a)} \\ \nabla \cdot \mathbf{u} &= 0 & \text{(5b)} \end{aligned}$$

$$\begin{aligned} \left(\partial_t - \frac{1}{Re_m}\right)\mathbf{B} - \nabla \times (\mathbf{u} \times \mathbf{B}) &= 0 & \text{(6a)} \\ \nabla \cdot \mathbf{B} &= 0 & \text{(6b)} \end{aligned}$$

where Re is the usual hydrodynamic Reynolds number and R_m the magnetic Reynolds number. To allow us to use (4) for both equations, we write (5a)-(6a) in the form:

$$\mathbf{f}_u \equiv \left(\partial_t - \frac{1}{Re}\Delta\right)\mathbf{u} + \mathbf{s}_u = -\nabla\left(p + B^2/2\right) \quad (7a)$$

$$\mathbf{g}_u \equiv \nabla \times \mathbf{f}_u = 0 \quad (7b)$$

$$\mathbf{g}_B \equiv \left(\partial_t - \frac{1}{Re_m}\Delta\right)\mathbf{B} + \mathbf{s}_B = 0 \quad (7c)$$

thus defining $\mathbf{g}_u$ and $\mathbf{g}_B$ which are both solenoidal. The decoupled evolution equations for the velocity potentials are derived by taking $\hat{\mathbf{e}}\cdot$ and $\hat{\mathbf{e}}\cdot\nabla\times$ of $\mathbf{g}_u$, i.e. $\hat{\mathbf{e}}\cdot\nabla\times$ and $\hat{\mathbf{e}}\cdot\nabla\times\nabla\times$ of $_{\mathbf{u}}$ Those for the magnetic potentials are derived by taking $\hat{\mathbf{e}}\cdot$ and $\hat{\mathbf{e}}\cdot\nabla\times$ of (6a). The evolution equations for the scalar potentials become:

$$(\partial_t - \frac{1}{Re}\Delta)\Delta_h\psi_u = \hat{\mathbf{e}}\cdot\nabla\times\mathbf{s}_u \quad (8a)$$

$$(\partial_t - \frac{1}{Re}\Delta)\Delta\Delta_h\phi_u = -\hat{\mathbf{e}}\cdot\nabla\times\nabla\times\mathbf{s}_u \quad (8b)$$

and

$$(\partial_t - \frac{1}{Re_m}\Delta)\Delta_h\phi_B = \hat{\mathbf{e}}\cdot\mathbf{s}_B \quad (9a)$$

$$(\partial_t - \frac{1}{Re_m}\Delta)\Delta_h\psi_B = \hat{\mathbf{e}}\cdot\nabla\times\mathbf{s}_B \quad (9b)$$

where

$$\mathbf{s}_u \equiv (\mathbf{u}\cdot\nabla)\mathbf{u} - (\mathbf{B}\cdot\nabla)\mathbf{B} \quad (10a)$$

$$\mathbf{s}_B \equiv -\nabla\times(\mathbf{u}\times\mathbf{B}) \quad (10b)$$

3 Conditions on velocity field

The velocity field is driven by the counter-rotation of the bounding disks. We have non-dimensionalized length by the radius and time by the inverse angular velocity. This leads to the boundary conditions:

$$\mathbf{u}|_{r=1} = 0, \quad (11a)$$

$$\mathbf{u}|_{z=\pm\frac{h}{2}} = \pm\, r\Omega\hat{\mathbf{e}}_\theta \quad (11b)$$

Although formally $\Omega = 1$ by our choice of units, we retain the possibility of a function $\Omega(r) \approx 1$ whose purpose is to regularize the boundary conditions which are otherwise discontinuous at $r = 1, z = \pm h/2$.

We now consider the number of boundary conditions required by equations (8) Equation (8a) is $2^{\rm nd}$ order in the vertical directions and $4^{\rm th}$ order in the horizontal directions. while equation (8b) is $4^{\rm th}$ order in the vertical directions and $6^{\rm th}$ order in the horizontal directions. A corresponding number of boundary conditions are required, a total of (2+4)/2=3 at each vertical boundary and (4+6)/2=5 at each horizontal boundary. These are provided by the 3 physical boundary conditions (11) for the velocity at the no-slip vertical and horizontal boundaries, which are to be supplemented by the gauge and compatibility conditions at the horizontal boundaries.

3.1 Hydrodynamic gauge condition

We begin by focusing on the hydrodynamic conditions and abbreviate $\phi \equiv \phi_u$, $\psi \equiv \psi_u$. In (1), ϕ is determined up to a solution of

$$\Delta_h \phi = 0 \tag{12}$$

while ψ is determined up to an arbitrary function of z. The gauge for the hydrodynamic potentials is chosen by fixing

$$\phi(r=1) = 0 \tag{13a}$$
$$\psi(r=0) = 0 \tag{13b}$$

3.2 Hydrodynamic boundary conditions

On the cylindrical surface $r=1$ we impose boundary conditions (11) on u_r, u_θ, u_z:

$$u_r = \frac{1}{r}\partial_\theta \psi + \partial_z \partial_r \phi = 0, \tag{14a}$$
$$u_\theta = -\partial_r \psi + \frac{1}{r}\partial_z \partial_\theta \phi = 0, \tag{14b}$$
$$u_z = -\Delta_h \phi = 0. \tag{14c}$$

The gauge choice (13a) can be used to simplify (14b):

$$\partial_\theta \phi = \partial_z \phi = 0 \quad \Longrightarrow \quad \partial_r \psi = 0 \tag{15}$$

On the simply-connected bounding disks $z = \pm h/2$, we can use the two-dimensional version of (4), which states that $\mathbf{u} \mp r\Omega \hat{\mathbf{e}}_\theta = 0$ is equivalent to:

$$0 = \hat{\mathbf{e}}_z \cdot \mathbf{u} = u_z = -\Delta_h \phi \tag{16a}$$
$$\frac{1}{r}\partial_r (r^2 \Omega_\pm) = \hat{\mathbf{e}}_z \cdot \nabla \times \mathbf{u} = \frac{1}{r}\left(\partial_r (r u_\theta) - \partial_\theta u_r\right) = -\Delta_h \psi \tag{16b}$$
$$0 = -\nabla_h \cdot \mathbf{u}_h = \partial_z u_z = -\partial_z \Delta_h \phi \tag{16c}$$

The remaining condition (4d) required at the two circular edges is insured by the imposition of (14a) on u_r. Equations (16) have the advantage of not coupling the potentials.

3.3 Hydrodynamic compatibility condition

The compatibility condition (4d) at $r = 1$ is

$$\begin{aligned} 0 = \hat{\mathbf{e}}_r \cdot \mathbf{g} = \hat{\mathbf{e}}_r \cdot \nabla \times \mathbf{f} &= \hat{\mathbf{e}}_r \cdot \nabla \times \left(\left(\partial_t - \frac{1}{Re}\Delta \right) \mathbf{u} + \mathbf{s} \right) \\ &= \left(\frac{1}{r}\partial_\theta \hat{\mathbf{e}}_z - \partial_z \hat{\mathbf{e}}_\theta \right) \cdot \left(\left(\partial_t - \frac{1}{Re}\Delta \right) \mathbf{u} + \mathbf{s} \right) \end{aligned} \tag{17}$$

Because derivatives ∂_θ and ∂_z act in directions parallel to the boundary $r = 1$, they vanish for all terms in $\mathbf{f}$ which are zero or constant at this boundary. For homogeneous boundary conditions (14) on the outer cylinder, this is true for $\partial_t \mathbf{u}$ and for $\mathbf{s}$ in the absence of a magnetic field. Then condition (17) takes the form:

$$0 = \frac{1}{r}\partial_\theta \Delta u_z - \partial_z \left(\left(\Delta - \frac{1}{r^2} \right) u_\theta + \frac{2}{r^2}\partial_\theta u_r \right) \tag{18}$$

Substituting the gauge condition (13a) and the relations between $\mathbf{u}$ and ψ, ϕ written in (14), we obtain:

$$0 = \partial_{rz}^2 \Delta_h \psi - \frac{1}{r}\partial_\theta \Delta \Delta_h \phi = 0 \tag{19}$$

4 Influence Matrix for Nested Elliptic Problems

The complete statement of the hydrodynamic problem is then:

$$(\partial_t - \frac{1}{Re}\Delta)\Delta_h \psi = \hat{\mathbf{e}}_z \cdot \nabla \times \mathbf{s} \equiv s_\psi \tag{20a}$$

$$(\partial_t - \frac{1}{Re}\Delta)\Delta\Delta_h \phi = -\hat{\mathbf{e}}_z \cdot \nabla \times \nabla \times \mathbf{s} \equiv s_\phi \tag{20b}$$

together with, at $r = 1$:

$$\frac{1}{r}\partial_\theta \psi + \partial_z \partial_r \phi = 0 \qquad (u_r) \tag{21a}$$

$$\partial_r \psi = 0 \qquad (u_\theta) \tag{21b}$$

$$\Delta_h \phi = 0 \qquad (u_z) \tag{21c}$$

$$\phi = 0 \qquad \text{(gauge)} \tag{21d}$$

$$\partial_{rz}^2 \Delta_h \psi - \frac{1}{r}\partial_\theta \Delta \Delta_h \phi = 0 \qquad \text{(compatibility)} \tag{21e}$$

and, at $z = \pm h/2$:

$$\Delta_h \psi = -\frac{1}{r}\partial_r (r^2 \Omega_\pm) \qquad (\hat{\mathbf{e}}_z \cdot \nabla \times \mathbf{u}_h) \tag{22a}$$

$$\partial_z \Delta_h \phi = 0 \qquad (\nabla_h \cdot \mathbf{u}_h) \tag{22b}$$

$$\Delta_h \phi = 0 \qquad (\hat{\mathbf{e}}_z \cdot \mathbf{u}) \tag{22c}$$

These high-order partial differential equations can be solved as nested Helmholtz and Poisson problems for:

$$\psi, \quad f_\psi \equiv \Delta_h \psi, \tag{23}$$

and

$$\phi, \quad f_\phi \equiv \Delta_h \phi, \quad g_\phi \equiv \Delta f_\phi \tag{24}$$

Ideally, each of the functions in (23), (24) would be subject to Dirichlet or Neumann boundary conditions, leading to a sequential solution procedure. This is close to, but not precisely, the case. Equation (21b) provides the necessary Neumann condition for ψ, (21d) the Dirichlet condition for ϕ, and (21c)-(22c) the Dirichlet conditions for f_ϕ. However (22a) provides a Dirichlet condition for f_ψ only at $z = \pm h/2$ and no simple boundary condition exists for g_ϕ. Conversely, conditions (21a), (21e) and (22b) must all be imposed. The *influence matrix method* – equivalent to Green's functions methods or decomposition into particular and homogeneous solutions – allows us to substitute the desired Dirichlet conditions for the exact conditions, and then to correct the resulting solution so that the exact conditions are satisfied.

We rewrite the complete problem (20)-(22) as follows:

$$(\partial_t - \frac{1}{Re}\Delta) f_\psi = s_\psi \tag{25a}$$

$$f_\psi = -\frac{1}{r}\partial_r (r^2 \Omega_\pm) \qquad \text{at } z = \pm h/2 \tag{25b}$$

$$\frac{1}{r}\partial_\theta \psi + \partial_z \partial_r \phi = 0 \Longleftrightarrow f_\psi = \sigma_{f_\psi}(z) \qquad \text{at } r = 1 \tag{25c}$$

$$\Delta_h \psi = f_\psi \tag{26a}$$

$$\partial_r \psi = 0 \qquad \text{at } r = 1 \tag{26b}$$

$$(\partial_t - \frac{1}{Re}\Delta) g_\phi = s_\phi \tag{27a}$$

$$\partial^2_{rz} f_\psi - \frac{1}{r}\partial_\theta g_\phi = 0 \Longleftrightarrow g_\phi = \sigma_{g_\phi}(z) \qquad \text{at } r = 1 \tag{27b}$$

$$\partial_z f_\phi = 0 \Longleftrightarrow g_\phi = \sigma_{g_\phi}(r) \qquad \text{at } z = \pm h/2 \tag{27c}$$

$$\Delta f_\phi = g_\phi \tag{28a}$$

$$f_\phi = 0 \qquad \text{at } r = 1 \tag{28b}$$

$$f_\phi = 0 \qquad \text{at } z = \pm h/2 \tag{28c}$$

$$\Delta_h \phi = f_\phi \tag{29a}$$

$$\phi = 0 \qquad \text{at } r = 1 \tag{29b}$$

The equations above require some explanation. The conditions shown on the left of the arrows in equations (25c), (27b) and (27c) cannot serve as Dirichlet or Neumann boundary conditions for a Helmholtz or Poisson problem. (Although the condition on the left in (27c) is a Neumann condition for f_ϕ, equations (28) already determine f_ϕ and a boundary condition for g_ϕ is lacking in problem (27).)

The influence matrix method calls for calculating σ_{f_ψ} and σ_{g_ϕ} such that the conditions on the left are satisfied. This is accomplished in the following way. In a preprocessing step, homogeneous versions ($s_\psi = s_\phi = 0$) of (25)-(29) are solved with all possible values σ_{f_ψ} and σ_{g_ϕ} for the inhomogeneous Dirichlet conditions. The resulting non-zero values of the operators to the left of the arrows are calculated. This yields the influence matrix, relating the conditions on the left- and right-hand-sides of the arrows. Note that the correspondence given in (25c), (27b) and (27c) serves only for counting purposes. In fact, the values of σ_{f_ψ} and σ_{g_ϕ} affect all of the values of the operators on the left-hand-sides of (25c), (27b) and (27c). Details can be found in [8, 1].

5 Temporal and spatial discretization; solution of Helmholtz and Poisson problems

We integrate the nonlinear terms by the explicit Adams-Bashforth formula and the Laplacian terms by the implicit backwards Euler formula. Thus, for example, (25a) is replaced by:

$$\left(I - \frac{\Delta t}{Re}\Delta\right) f_\psi = \frac{\Delta t}{2}\left(3 s_\psi^n - s_\psi^{n-1}\right) \tag{30}$$

We use the pseudospectral method [9] to discretize our fields. In the θ and z directions we use Fourier modes and Chebyshev polynomials. In the radial direction, we use a polynomial basis developed by Matsushima and Marcus [10] which is regular at the axis. Thus

$$f(r,\theta,z) \approx \sum_{m=-\left\lfloor \frac{M}{2} \right\rfloor}^{\left\lfloor \frac{M}{2} \right\rfloor} \sum_{k=0}^{K-1} \sum_{\substack{n=|m| \\ n+m \text{ even}}}^{\hat{N}} \hat{f}_{kn}^m e^{im\theta} \mathcal{Q}_n^m(r) \mathcal{T}_k\left(\frac{2z}{h}\right) \tag{31}$$

where $\hat{f}_{kn}^m$ are complex coefficients, $\mathcal{T}_k$ are Chebyshev polynomials and $\mathcal{Q}_n^m$ are the Matsushima-Marcus radial functions. We have run the hydrodynamic code for $h = 2$ (height = diameter) and Reynolds numbers up to 5000, for which the resolution requirements are $\Delta t = 0.001$ and $M \times K \times N = 96 \times 128 \times 80$. In order to solve the Helmholtz and Poisson problems (25)–(29), we diagonalize in the θ and z directions to reduce the equations to a set of one-dimensional problems in the radial direction, which we then solve by the use of recursion relations [10, 11]. Details can be found in [8, 10].

6 Conditions on magnetic field

We now turn to the formulation of the magnetic problem, abbreviating its scalar potentials as ϕ and ψ. We consider the cylinder to be surrounded by an external vacuum, in which the magnetic field obeys:

$$\mathbf{B}^{vac} = \nabla\phi^{vac} \tag{32a}$$

$$\Delta\phi^{vac} = 0 \tag{32b}$$

$$\mathbf{B}^{vac}|_{(r,z)\to\infty} = 0 \tag{32c}$$

but is otherwise not fixed. The magnetic field is required to be continuous at the cylinder boundary:

$$[\mathbf{B}]_\partial \equiv \mathbf{B}|_{\partial\Omega} - \mathbf{B}^{vac}|_{\partial\Omega} = 0 \tag{33}$$

Equations (39) constitute three conditions at the boundary for the three potentials ψ^B, ϕ^B and ϕ^{vac}. In section , we will discuss a method for imposing these conditions.

Equations (9a) and (9b) are both 2^{nd} order in the vertical directions and 4^{th} order in the horizontal directions and require (2+2)/2=2 conditions at each vertical boundary and (4+4)/2=4 at each horizontal boundary. Since the physical boundary conditions are matching conditions with the external magnetic field, the number of unknown scalar fields increases from 2 to 3, as does the number of conditions (33) at the interface. As in the hydrodynamic case, these conditions are to be supplemented by gauge and compatibility conditions at the horizontal boundaries.

6.1 Magnetic compatibility condition

The magnetic compatibility condition (4d) can be derived in an analogous way to that of the velocity:

$$\hat{\mathbf{e}}_r \cdot \mathbf{g}_B = \hat{\mathbf{e}}_r \cdot \left(\left(\partial_t - \frac{1}{Rm}\Delta \right) \mathbf{B} + \mathbf{s}_B \right) = 0 \tag{34}$$

Here, several differences appear. Contrary to the velocity, the magnetic field does not vanish on the boundary so $\partial_t \mathbf{B} \neq 0$. The nonlinear term

$$\mathbf{s}_B = \hat{\mathbf{e}}_r \cdot \nabla \times (\mathbf{u} \times \mathbf{B})|_{r=1} \tag{35}$$

vanishes at the boundary when $\mathbf{u}|_{r=1} = 0$ is imposed. (Note that normal derivatives of $\mathbf{u}$, which are generally not zero at $r = 1$, do not appear in (35).)

$$\hat{\mathbf{e}}_r \cdot \left(\partial_t - \frac{1}{Rm}\Delta\mathbf{B} \right) = 0 \tag{36}$$

In polar coordinates the radial component of the vector Laplace operator has the following form

$$\hat{\mathbf{e}}_r \cdot \Delta\mathbf{B} = \left(\Delta - \frac{1}{r^2} \right) B_r - \frac{2}{r^2}\partial_\theta B_\theta \tag{37}$$

Using (37) and substituting the potential form of B_r and B_θ we obtain the potential form of the magnetic compatibility condition at $r = 1$:

$$\left(\partial_t - \frac{1}{Rm}\left(\Delta - \frac{1}{r^2}\right)\right)\underbrace{\left(\frac{1}{r}\partial_\theta\psi + \partial_r\partial_z\phi\right)}_{B_r} + \frac{1}{Rm}\frac{2}{r^2}\partial_\theta\underbrace{\left(-\partial_r\psi + \frac{1}{r}\partial_z\partial_\theta\phi\right)}_{B_\theta} = 0 \qquad (38)$$

6.2 Magnetic gauge conditions and statement of matching conditions

In terms of cylindrical coordinates and potentials, the matching conditions are written as:

$$0 = B_r - B_r^{vac} = \frac{1}{r}\partial_\theta\psi + \partial_r\left(\partial_z\phi - \phi^{vac}\right) \qquad (39a)$$

$$0 = B_\theta - B_\theta^{vac} = -\partial_r\psi + \frac{1}{r}\partial_\theta\left(\partial_z\phi - \phi^{vac}\right) \qquad (39b)$$

$$0 = B_z - B_z^{vac} = -\Delta\phi + \partial_z\left(\partial_z\phi - \phi^{vac}\right) \qquad (39c)$$

The matching conditions (39) suggest the choice of

$$\left(\partial_z\phi - \phi^{vac}\right)|_{r=1} = 0 \qquad (40)$$

as a gauge for ϕ. Equation (40) can be differentiated along the bounding cylinder, i.e. in z and θ. Using (40), the matching conditions at $r = 1$ (but not at $z = \pm h/2$) are then simplified to:

$$0 = \frac{1}{r}\partial_\theta\psi + \partial_r\left(\partial_z\phi - \phi^{vac}\right) \qquad (41a)$$

$$0 = \partial_r\psi \qquad (41b)$$

$$0 = \Delta\phi \qquad (41c)$$

At $z = \pm h/2$, we may impose the matching conditions in the same form as in (16)

$$0 = \hat{\mathbf{e}}_z \cdot [\mathbf{B} - \mathbf{B}^{vac}] = -\Delta\phi + \partial_z\left(\partial_z\phi - \phi^{vac}\right) \qquad (42a)$$

$$0 = \hat{\mathbf{e}}_z \cdot \nabla \times [\mathbf{B} - \mathbf{B}^{vac}] = \hat{\mathbf{e}}_z \cdot \nabla \times \mathbf{B} = \Delta_h\psi \qquad (42b)$$

$$0 = \nabla_h \cdot [\mathbf{B} - \mathbf{B}^{vac}] = \partial_z[B_z - B_z^{vac}] = \partial_z[-\Delta_h\phi - \partial_z\phi^{vac}] \qquad (42c)$$

The coupling with the external field ϕ^{vac} has been reduced relative to (39) but not eliminated. The remainder of the paper is devoted to exploring a method for imposing boundary conditions (41)–(42) without the necessity for solving the external Laplace equation (32b).

7 Magnetic boundary conditions

7.1 Matching to an external harmonic solution: Green's functions

We are interested in solving the following scalar potential problem:

$$\Delta\Phi(\mathbf{x}) = \rho(\mathbf{x}) \quad ; \quad \mathbf{B} = \nabla\Phi \quad \text{and} \quad \mathbf{B}(|\mathbf{x}| \to \infty) \to 0 \qquad (43)$$

where Φ is a scalar potential of a vector potential field $\mathbf{B}$ which we require to vanish at an infinite distance from the field sources ρ located inside a bounded region Ω so that:

$$\rho(\mathbf{x}) = \begin{cases} \rho(\mathbf{x}') & \mathbf{x}' \equiv \mathbf{x} \in \Omega \\ 0 & \mathbf{x} \notin \Omega \quad \text{or} \quad \mathbf{x} \in \Omega^* \equiv \mathcal{D} - \Omega \end{cases} \tag{44}$$

where $\mathcal{D}$ is a global domain and Ω is a bounded sub-domain with boundary $\partial\Omega$. A physical interpretation of (43) can be an electrostatic potential Φ of a field $\mathbf{F}$ generated by charges distributed in space with the density ρ.

A possible way of solving (43)–(44) is to build the solution from the fundamental solutions of the Laplace equation. This construction protocol corresponds to a well-known Green function method. It follows from the linearity of the Laplace equation that any harmonic function can be constructed using a fundamental solutions (or Green function) satisfying

$$\Delta G(\mathbf{x}; \mathbf{x}') = \delta(|\mathbf{x} - \mathbf{x}'|) \tag{45}$$

In three dimensions the Green function for the Laplace equation is $G(\mathbf{x}; \mathbf{x}') = -\frac{1}{4\pi}|\mathbf{x} - \mathbf{x}'|^{-1}$ and in the electrostatic context corresponds to the potential of an isolated point charge. In two dimensions we have $G(\mathbf{x}; \mathbf{x}') = -\frac{1}{4\pi}\ln|\mathbf{x} - \mathbf{x}'|$. Using *Green's second identity* one can show [12] that solutions to (43) can be written as:

$$\Phi(\mathbf{x}) = \frac{1}{4\pi\epsilon_0}\int_\Omega \rho(\mathbf{x}')G(\mathbf{x}; \mathbf{x}')\, d^3x' + \frac{1}{4\pi}\oint_{\partial\Omega}\left(G(\mathbf{x}; \mathbf{x}')\frac{\partial\Phi(\mathbf{x}')}{\partial n'} - \Phi(\mathbf{x}')\frac{\partial G(\mathbf{x}; \mathbf{x}')}{\partial n'}\right) da' \tag{46}$$

where the volume integral ensures satisfaction of the equation while the surface integral, corresponding to a harmonic part of the solution, can be used to impose the boundary conditions for the problem.

Equation (46) is in fact already a recipe for how to impose the boundary conditions for the solution in the internal domain Ω. so that it is harmonic on the boundary. If one incorporates the integral boundary condition (46) into a solver, then the internal solution is guaranteed to match the external harmonic part of the solution. Equation (46) with $\rho(\mathbf{x}) = 0$ is an integral equation of the second kind with a singular (but integrable) kernel and can be solved numerically by specialized methods (see [13]). This approach has been implemented by Isakov *et al.* [14] using a integro-differential formulation in which the finite volume method is used in the internal region and the *boundary element method* is used to discretize the solution at the boundary. The authors show that the integral equation on the boundary can be solved efficiently at a cost of $O(N^2)$ operations (for a finite boundary element method), where N^2 is the total number of boundary points. We wish to formulate an analogous method for our spatial spectral discretisation, described in section 5.

7.2 Influence matrix method

Instead of ensuring that the internal solution be harmonic on the boundary by implementing condition (46) directly, we shall use the influence matrix methodology to make sure that the

internal solution smoothly matches a harmonic function satisfying appropriate asymptotic conditions at infinity. This is equivalent to imposing (46). We shall denote the external harmonic solution by $\phi(\mathbf{x})$ while $\Phi(\mathbf{x})$ will stand for the internal solution. The two-domain problem is described by the following system of equations:

$$\Delta\Phi = \rho \qquad \Delta\phi = 0 \tag{47}$$

with boundary conditions

$$\begin{aligned} \Phi(\mathbf{x}) - \phi(\mathbf{x}) &= 0 \qquad \mathbf{x} \in \partial\Omega && \text{(48a)} \\ \partial_n\Phi(\mathbf{x}) - \partial_n\phi(\mathbf{x}) &= 0 \qquad \mathbf{x} \in \partial\Omega && \text{(48b)} \\ \phi(\mathbf{x}) &\to 0 \qquad |\mathbf{x}| \to \infty && \text{(48c)} \end{aligned}$$

To implement the continuity conditions (48a)–(48b) one does not need to know the external solution. It is enough to know a harmonic basis $\{\mathcal{H}_n(\mathbf{x})\}$ in which $\phi(\mathbf{x})$ can be represented:

$$\phi(\mathbf{x}) = \sum_n \beta_n \mathcal{H}_n(\mathbf{x}) \tag{49}$$

In order to separate the problem of satisfaction of the internal equation from that of imposing the boundary conditions (48a)–(48b), we decompose the internal solution Φ into particular and homogeneous parts so that $\Phi = \Phi^p + \Phi^h$ and

$$\begin{aligned} \Delta\Phi^p &= \rho & \Delta\Phi^h &= 0 \\ \Phi^p|_{\partial\Omega} &= 0 & \Phi^h|_{\partial\Omega} &\neq 0 \end{aligned} \tag{50}$$

In writing (50), we assume that we dispose of a solver able to solve Poisson's equation with any specified boundary values. The role of Φ^p is to satisfy the Poisson equation, while that of Φ_h is to ensure the satisfaction of (48a)–(48b). We can compute a set of linearly independent homogeneous solutions $\{\Phi^h_n\}$ so that Φ^h can be written as $\Phi^h(\mathbf{x}) = \sum_n \alpha_n \Phi^h_n(\mathbf{x})$. The matching conditions for can now be written as:

$$\Phi(\mathbf{x}) - \phi(\mathbf{x}) = \Phi^p(\mathbf{x}) + \sum_m \left[\alpha_m \Phi^h_m(\mathbf{x}) - \beta_m \mathcal{H}^h_m(\mathbf{x})\right] = 0 \tag{51a}$$

$$\frac{\partial\Phi}{\partial n}(\mathbf{x}) - \frac{\partial\phi}{\partial n}(\mathbf{x}) = \frac{\partial\Phi^p}{\partial n}(\mathbf{x}) + \sum_m \left[\alpha_m \frac{\partial\Phi^h_m}{\partial n}(\mathbf{x}) - \beta_m \frac{\partial\mathcal{H}^h_m}{\partial n}(\mathbf{x})\right] = 0 \tag{51b}$$

where Φ^p, Φ^h_m, $\mathcal{H}_m$ are known, so (51) defines a linear system of equations for the unknown coefficients $\{\alpha_m, \beta_m\}$. These equations must be satisfied at each boundary point $\mathbf{x} \equiv \mathbf{x}_k$. This can be written in matrix form as follows:

$$\underbrace{\left[\begin{array}{c|c} \mathbf{A} & \mathbf{B} \\ \hline \mathbf{C} & \mathbf{D} \end{array}\right]}_{\mathbf{M}} \left[\begin{array}{c} \alpha \\ \hline \beta \end{array}\right] = \left[\begin{array}{c} 0 \\ \hline \mathbf{P} \end{array}\right] \tag{52}$$

where $\mathbf{A} \equiv \Phi^h_m(\mathbf{x}_k)$, $\mathbf{B} \equiv -\mathcal{H}_m(\mathbf{x}_k)$, $\mathbf{C} \equiv \partial_n \Phi^h_m(\mathbf{x}_k)$, $\mathbf{D} \equiv -\partial_n \mathcal{H}^h_m(\mathbf{x}_k)$, $\alpha \equiv \alpha_n$, $\beta \equiv \beta_n$ and $\mathbf{P} \equiv -\partial_n \Phi^p(\mathbf{x}_k)$. The matrix $\mathbf{M}$ is called the *influence matrix*. The cost of creating and inverting of the influence matrix can be significant. It is therefore not economical to use this method if the solution must be found only once. This is not the case, however, if one needs to solve (43-44) repeatedly, as is the case when the Poisson problem is solved at each time step of a time-dependent simulation, because the influence matrix can be computed once in a preprocessing step. The cost can be further decreased by performing a *Schur decomposition* of the influence matrix:

$$\mathbf{C}\alpha + \mathbf{D}\beta = \mathbf{P} \qquad \Longrightarrow \beta = \mathbf{D}^{-1}(\mathbf{P} - \mathbf{C}\alpha) \tag{53a}$$

$$\mathbf{A}\alpha + \mathbf{B}\beta = 0 \qquad \Longrightarrow (\mathbf{A} - \mathbf{B}\mathbf{D}^{-1}\mathbf{C})\alpha = -\mathbf{B}\mathbf{D}^{-1}\mathbf{P} \tag{53b}$$

reducing its dimension by a factor of two and effectively eliminating completely the external solution from the problem.

7.3 Construction of a harmonic basis

Matching the internal solution with the external one requires the knowledge of a harmonic basis $\mathcal{H}_m$. The spherical harmonics, while a valid basis, are usable in practice only if the domain boundary is spherical, since they converge badly near a non-spherical boundary. One needs a basis of harmonic functions constructed in accordance to the boundary shape which represents uniformly the field on the boundary. In the following we present a method for constructing a well-behaved harmonic basis $\mathcal{H}_m$.

From now on we will limit ourselves to a two-dimensional problem, motivated by the idea that this is a necessary first step toward deriving a three-dimensional algorithm. All the key problems which we have described in the case of a non-spherical boundary in three dimensions are also present in two dimensions for a non-circular domain. For simplicity and in view of future application to a spectral solver we will consider Ω to be a rectangular region.

We wish to construct a basis set of harmonic functions, each of which takes on specified values $f(x)$ along one side of the rectangle. We can use the Green function $G(\mathbf{x};\mathbf{x}')$ to do this. Since each side of the rectangle is a finite interval $a \le x \le b = a + H$, we can write the following one-dimensional problem:

$$\int_a^b G(x;x')\,\sigma(x')\,dx' = f(x) \tag{54}$$

where $\sigma(x)$ is a source distribution on the line which generates potential equal to $f(x)$ for $x \in [a,b]$. Equation (54) is a Fredholm integral equation of the first kind for $\sigma(x)$, a class of inverse problems which is in general ill-posed or ill-conditioned. However, it can be solved for kernels which are Green functions of the Laplace equation. In two dimensions, we have $G \sim \ln|\mathbf{x} - \mathbf{x}'|$ so that (54) becomes

$$\int_a^b \ln|x - x'|\,\sigma(x')\,dx' = f(x) \tag{55}$$

This equation is known as Carleman's equation and has the following solution [15]:

$$\sigma(x) = \frac{1}{\pi^2\sqrt{(x-a)(b-x)}}\left[\int_a^b \frac{\sqrt{(t-a)(b-t)}f'(t)\,dt}{t-x} + \frac{1}{\ln(H/4)}\int_a^b \frac{f(t)\,dt}{\sqrt{(t-a)(b-t)}}\right] \tag{56}$$

if $H \neq 4$.

We use Chebyshev polynomials to represent the internal solutions, and therefore take as boundary values $f(x)$ each of the functions $\mathcal{T}_n(2x/H) \equiv \cos(n\,\arccos(2x/H))$. The corresponding solutions $\sigma_n(x)$ are:

$$\sigma_n(x) = A_n\frac{\mathcal{T}_n(2x/H)}{\pi\sqrt{\left(\frac{H^2}{4}-x^2\right)}} \quad ; \quad A_n = \begin{cases} -n & n>0 \\ [\ln(H/4)]^{-1} & n=0 \end{cases} \tag{57}$$

Because the different $\mathcal{T}_n$'s form an orthogonal basis for all possible boundary value distributions on the segment of length H, then through (46) they also define a basis for all two-dimensional harmonic solutions having this segment as a boundary.

Let us consider a rectangular domain $[-H/2, H/2] \times [-1, 1]$. Assuming that our segment lies along the x direction, then a two-dimensional potential $\phi_n^x(\mathbf{x})$ has the following form:

$$\phi_n^x(\mathbf{x}) = \int_{-H/2}^{H/2} \ln\,|\mathbf{x} - x'\hat{\mathbf{e}}_x|\,\sigma_n(x')\,dx' \tag{58}$$

Some of these harmonic functions are illustrated in figure 2. For a harmonic function with specified values along a segment in the y direction, we have:

$$\phi_m^y(\mathbf{x}) = \int_{-1}^{1} \ln\,|\mathbf{x} - y'\hat{\mathbf{e}}_y|\,\sigma_m(y')\,dy' \tag{59}$$

Any external harmonic function can then be approximated by the following truncated series:

$$\begin{aligned}\phi^{N,M}(\mathbf{x}) = &\sum_{n=0}^{N-1}\left[c_n^{x,-}\phi_n^x\left(\mathbf{x}+\frac{H}{2}\hat{\mathbf{e}}_x\right) + c_n^{x,+}\phi_n^x\left(\mathbf{x}-\frac{H}{2}\hat{\mathbf{e}}_x\right)\right] \\ &+ \sum_{m=0}^{M-1}\left[c_m^{y,-}\phi_m^y\left(\mathbf{x}+1\hat{\mathbf{e}}_y\right) + c_m^{y,+}\phi_m\left(\mathbf{x}-1\hat{\mathbf{e}}_y\right)\right]\end{aligned} \tag{60}$$

The potential $\phi(\mathbf{x})$ of (60) is defined by the $2(N+M)$ coefficients $\{c_n^{x,-}, c_n^{x,+}, c_m^{y,-}, c_m^{y,+}\}$. If the solution $\Phi(\mathbf{x})$ in the internal domain Ω is represented with spectral resolution $N \times M$ via

$$\Phi^{N,M}(\mathbf{x}) = \sum_{n=0}^{N-1}\sum_{m=0}^{M-1} T_n(2x/H)T_m(y) \tag{61}$$

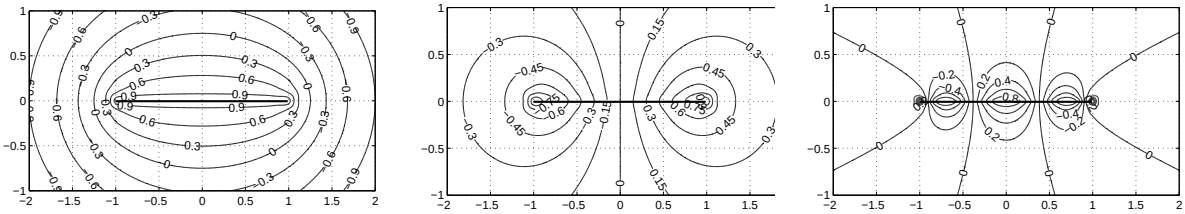

Figure 2: Potentials $\phi_n^x(\mathbf{x})$ generated by line source distributions $\sigma_n(x)$ with $H = 2$. Values of the potentials on the line segment $x \in [-1, 1]$ correspond to the Chebyshev polynomials $\mathcal{T}_n(x)$. Figures present (from left to right): $\sigma_0(x)$, $\sigma_1(x)$, $\sigma_4(x)$.

then the total number of linearly independent boundary value distributions of the internal solution $\Phi^{N,M}$ equals the number of basis functions forming the external solution $\phi^{N,M}$ and the matching can be accomplished by solving a linear system of equations, applying the influence matrix protocol described in the previous section. The basis functions $\{\phi_n^x, \phi_m^y\}$ of (58)–(59) (unlike the spherical harmonic basis) lead to a well-conditioned linear system, so the method can be applied to high spectral resolutions.

The harmonic functions $\phi_n^x(\mathbf{x})$ and $\phi_m^y(\mathbf{x})$ can be evaluated by performing integrations (58)–(59) numerically. Special attention must be paid during this process since both the kernel $G(\mathbf{x}; x')$ and the density $\sigma(x')$ have integrable singularities within the domain of integration. The singular points are $x'\hat{\mathbf{e}}_x = \mathbf{x}$ and $x' = \pm H/2$ for ϕ_n^x and $y'\hat{\mathbf{e}}_y = \mathbf{x}$ and $y' = \pm 1$ for ϕ_m^y. Dedicated adaptive quadratures (see [16]) can be used to compute these integrals accurately. When the normal derivatives of $\phi_n(\mathbf{x})$ need to be evaluated, only the integral kernel is differentiated. For $G(\mathbf{x}; x') \equiv \ln\,|\mathbf{x} - x'\hat{\mathbf{e}}_x|$ one obtains

$$\frac{\partial \phi_n^x}{\partial n}(x, y) = \frac{\partial}{\partial y} \int_{-H/2}^{H/2} \frac{1}{2} \ln\,\left[(x - x')^2 + y^2\right] \sigma_n(x')\, dx' = \int_{-H/2}^{H/2} \frac{y}{(x - x')^2 + y^2} \sigma_n(x')\, dx' \tag{62}$$

8 Validation of matching method: electrostatic example

We apply our method to a simple problem from electrostatics. For a given distribution of electric charges ρ_m:

$$\rho_m(r, \theta) = r^m e^{-r^2/\delta^2} \cos(m\theta) \qquad r \equiv |\mathbf{x}| = \sqrt{x^2 + y^2},\ \ \theta \equiv \arg(x + iy) \tag{63}$$

confined in a rectangular domain but localized around the coordinate origin $x = y = 0$, we seek the corresponding electric potential. The r^m factor in (63) ensures regularity of ρ_m at $r = 0$. The parameter δ is chosen to make ρ_m very small near the boundaries. We expect that the solution should be almost unaffected by the presence of boundaries and, for $\rho_{m=0}(r, \theta)$, should lead to an axisymmetric solution. Figure 3 shows the numerical result obtained using $\delta^2 = 0.15$ for the spectral resolution $N = 8$ in both directions. The domain boundary is represented by a bold square. One can see that the presence of the boundaries has minimal effect on the contours, which are almost perfectly circular as should be the case for δ small.

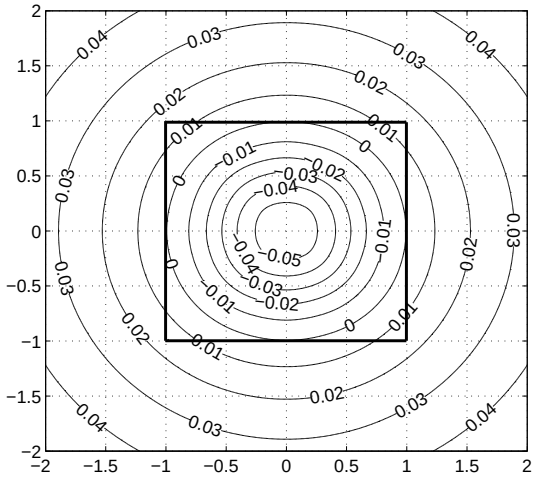

Figure 3: Potential $\Phi_{m=0}^{N=8}$ generated by sources (63) for $\delta = 0.15$. The maximal relative error for this numerical solution is $E_{m=0}(N = 8) \approx 0.03$. An analytic solution is given by (64a).

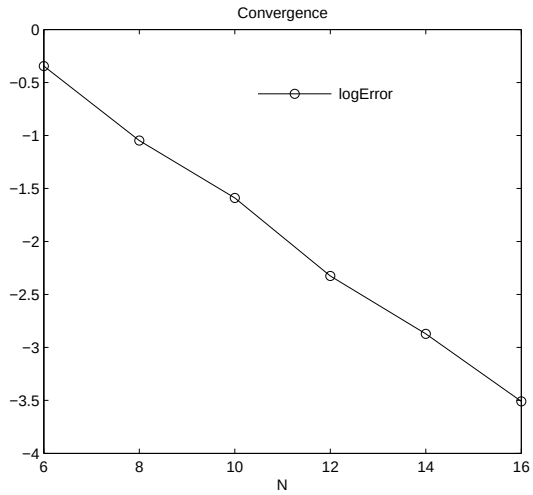

Figure 4: Convergence test: $\log_{10} E_{m=0}(N)$ (eq. (65)) is plotted for $N = [6, \ldots, 16]$, $\delta^2 = 0.1$.

The potential due to unbounded sources (not restricted to the internal domain) defined by (63) can be found analytically. For $m = \{0, 1, 2\}$ we have:

$$\Phi_{m=0}(r,\theta) = \frac{\delta^2}{4}\left[Ei\left(1, \frac{r^2}{\delta^2}\right) + 2\log(r)\right] \tag{64a}$$

$$\Phi_{m=1}(r,\theta) = \frac{\delta^4}{4r}\left[e^{-\frac{r^2}{\delta^2}} - 1\right]\cos\theta \tag{64b}$$

$$\Phi_{m=2}(r,\theta) = \frac{\delta^4}{4r^2}\left[\left(\delta^2 + r^2\right)e^{-\frac{r^2}{\delta^2}} - \delta^2\right]\cos 2\theta \tag{64c}$$

where $Ei(a,z) = \int_1^\infty e^{-tz}t^{-a}\,dt$ is the *error function* and we selected $\Phi_0,\ \Phi_1$ having finite values at $r = 0$. To evaluate the error convergence of the method we computed the relative error $E_m(N)$ defined as

$$E_m(N) = \sup_{r,\theta} \frac{|\Phi_m(r,\theta) - \Phi_m^N(r,\theta)|}{|\Phi_m(r,\theta)|} \tag{65}$$

where $\Phi_m^N(r,\theta)$ is the solution computed numerically with spectral resolution N in both spatial directions. Figure 4 proves the exponential convergence of the method. We tested our method for different source distributions and in each case we observed exponential convergence toward the analytic solution (64c). Figures 5–6 show the electric potentials $\Phi_{m=1}^{N=16}$ and $\Phi_{m=2}^{N=16}$. Convergence can only be confirmed up to a limited precision since the analytic solution (64c) corresponds to an unbounded source distribution, and not to the problem we are solving numerically in which sources are confined to the internal rectangle. The best agreement can be achieved for small values of δ. If the numerical solution with highest spectral resolution (here

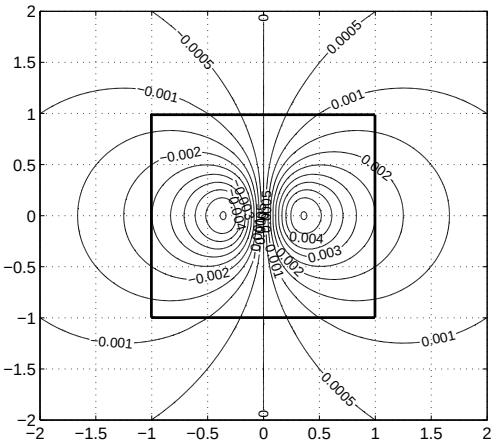

Figure 5: Potential $\Phi_{m=1}^{N=16}$ generated by sources (63) for $\delta = 0.1$. The analytic solution is given by (64b).

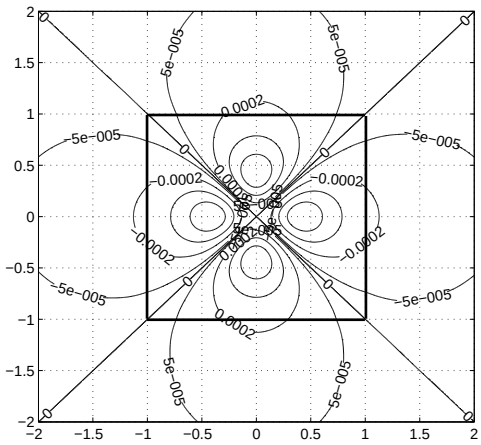

Figure 6: Potential $\Phi_{m=2}^{N=16}$ generated by sources (63) for $\delta = 0.1$. The analytic solution is given by (64c).

$N = 64$) is instead taken as a reference, then the method converges to this solution spectrally up to machine precision. Finally, one can see on figure 7 the effect of sources situated near the boundary.

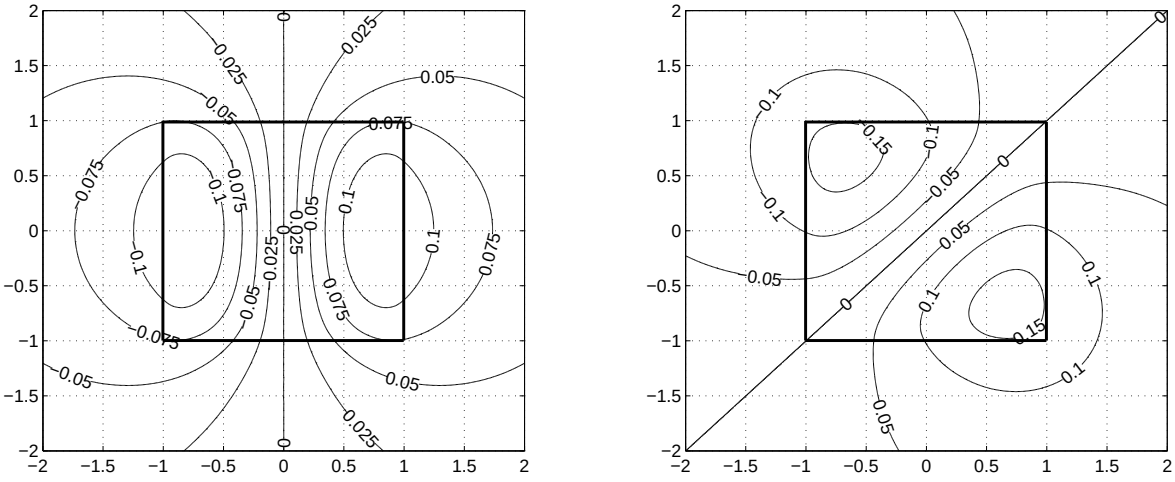

Figure 7: Potential $\Phi_{m=1}^{N=16}$ generated by sources (63) for $\delta = 2$. In the figure on the right, the dipole source distribution has been rotated by 45° about the origin. For this large value of δ, charges are located near the boundary.

9 Conclusions and perspectives

We have formulated a method for solving the hydrodynamic equations in a finite cylinder in which the velocity field is represented by two scalar fields and are divergence-free by construction. Although the poloidal-toroidal decomposition leads to an increase in the order of

the governing equations and in the number and complexity of conditions that must be imposed at the boundary, we have shown that these obstacles can be overcome by use of the influence matrix method.

The poloidal-toroidal decomposition can also be applied to the magnetic field and to the coupled magnetohydrodynamic equations. Because the induction equation conserves divergence, the order of the equations is lower. However, the compensating complication is that the values of the magnetic field on the boundary are unknown; instead, the field must be matched to an external field. In order to formulate a method for imposing these conditions, we have investigated a simpler problem which shares many of the same features: a two-dimensional Poisson equation in a bounded rectangular domain. The solution and its normal derivative are required to match those of a harmonic function which decays at infinity in an external domain.

We have developed a method using Green functions which solves only the internal problem and determines the boundary conditions ensuring smooth matching with the external solution. The new and essential element of this approach is the construction of a basis of harmonic functions which represent the near-boundary external solutions uniformly and is adapted to a spectral discretisation of the internal domain. This basis is used for constructing the influence matrix, which serves to impose the coupled boundary conditions between the internal and external solutions. The method is numerically well conditioned and can be used for high spatial resolutions. For a spectral solver, this method guarantees exponential convergence. This method might seem computationally expensive, but the most costly process – construction of a basis of external harmonic functions – is performed only once, and so its cost is a negligible component of a long-time integration.

Future work will focus on adapting the method to the three-dimensional magnetohydrodynamic equations in a finite cylinder where the poloidal-toroidal decomposition can be used. Since the cylindrical coordinates have one periodic direction it should be possible to apply this method separately to each of the Fourier modes treated individually as two-dimensional problems.

REFERENCES

[1] L.S. Tuckerman, Divergence-free velocity fields in nonperiodic geometries. *J. Comput. Phys.* **80**, 403–441 (1989).

[2] J.U. Brackbill & D.C. Barnes, The effect of nonzero $\div \mathbf{B}$ on the numerical solution of the magnetohydrodynamic equations. *J. Comput. Phys.* **35** 426 (1980).

[3] M. Dudley & R. James, Time-dependent kinematic dynamos with stationary flows. *Proc. Roy. Soc. London A* **425**, 407–429 (1989).

[4] R. Hollerbach, A spectral solution of the magneto-convection equations in a spherical geometry. *Int. J. Numer. Meth. Fluids* **32**, 773–797 (2000).

[5] J. Kim, P. Moin & R. Moser, Turbulence statistics in fully developed channel flow. *J. Fluid Mech.* **177**, 133–166 (1987).

[6] F. Marques, On boundary conditions for velocity potentials in confined flows: Application to Couette flow. *Phys. Fluids A* **2**, 729 (1990).

[7] F. Marques, M. Net, J. Massaguer, & I. Mercader, Thermal convection in vertical cylinders. A method based on potentials. *Computer Methods in Applied Mechanics and Engineering* **110**, 157 (1993).

[8] P. Boronski, A method based on poloidal-toroidal potentials applied to the von Kármán flow in a finite cylindrical geometry. Ph.D Thesis, Ecole Polytechnique, 2005.

[9] C. Canuto, M. Y. Hussaini, A. Quarteroni, T. A. Zang 1988 *Spectral Methods in Fluid Dynamics*. Springer-Verlag, New York.

[10] T. Matsushima, & P.S. Marcus, A spectral method for polar coordinates. *J. Comput. Phys.* **120**, 365–374 (1995).

[11] L.S. Tuckerman, Transformation of matrices into banded form. *J. Comput. Phys.* **84**, 360–376 (1989).

[12] J. D. Jackson, *Classical Electrodynamics*, 3rd ed., Wiley (1999).

[13] V. Rokhlin V., Rapid solution of integral equations of classical potential theory. *J. Comp. Phys.* **60**, 187–207 (1985).

[14] A. B. Iskakov, S. Descombes & E. Dormy, An integro-differential formulation for magnetic induction in bounded domains: boundary element-finite volume method. *J. Comput. Phys.* **197**, 540–554. (2004).

[15] A. D. Polyanin & A. V. Manzhirov, *Handbook of Integral Equations*, CRC Press (1998).

[16] W.H. Press, B.P. Flannery, S.A. Teukolsky & W.T. Vetterling, *Numerical Recipes: The Art of Scientific Computing*, Cambridge Univ. Press (1986).